



HAL
open science

Introduction of milled kaolinite obtained by mechanosynthesis to cement mixture for the production of mortar: Study of mechanical performance of modified mortar

Rabah Hamzaoui, Othmane Bouchenafa, Oumeima Ben Maaouia, Sofiane
Guessasma

► To cite this version:

Rabah Hamzaoui, Othmane Bouchenafa, Oumeima Ben Maaouia, Sofiane Guessasma. Introduction of milled kaolinite obtained by mechanosynthesis to cement mixture for the production of mortar: Study of mechanical performance of modified mortar. Powder Technology, 2019, 355, pp.340-348. 10.1016/j.powtec.2019.07.062 . hal-02545427

HAL Id: hal-02545427

<https://hal.inrae.fr/hal-02545427>

Submitted on 25 Oct 2021

HAL is a multi-disciplinary open access archive for the deposit and dissemination of scientific research documents, whether they are published or not. The documents may come from teaching and research institutions in France or abroad, or from public or private research centers.

L'archive ouverte pluridisciplinaire **HAL**, est destinée au dépôt et à la diffusion de documents scientifiques de niveau recherche, publiés ou non, émanant des établissements d'enseignement et de recherche français ou étrangers, des laboratoires publics ou privés.



Distributed under a Creative Commons Attribution - NonCommercial 4.0 International License

1 **Introduction of milled kaolinite obtained by mechanosynthesis to cement**
2 **mixture for the production of mortar: Study of mechanical performance of**
3 **modified mortar**

4 **Rabah Hamzaoui^{*1}, Othmane Bouchenafa¹, Oumeima Ben Maaouia¹, Sofiane**
5 **Guessasma².**

6 ¹ Université Paris-Est, Institut de Recherche en Constructibilité, ESTP, 28 avenue du
7 Président Wilson, 94234 Cachan, France

8 ² INRA, Research Unit BIA UR1268, Rue Géraudière, F-44316 Nantes, France

9 *: Correspondent author: rhamzaoui@estp-paris.eu

10 **Abstract**

11 The effect of the substitution by 5%, 15%, 30% and 45% of cement in mortars by milled
12 kaolinite has been studied. Milled Kaolinite clay is obtained by using planetary ball mill. The
13 influence on the mechanical performance and on the pozzolanic reactions are discussed. For
14 both CEM I and CEM II formulations, after only 7 days of curing, the compression strength
15 of mortars with 5% of milled kaolinite is comparable to the one of reference mortars for
16 milling times of 3 hours and above. For CEM I mortar, the results of the compressive strength
17 show that 15% of kaolinite milled for 9h allows the best compressive gain for 28 curing days
18 and 90 curing days with 18.5% and 25.6%, respectively. For CEM II mortar, 15% of kaolinite
19 milled for 9h exhibits the best values of compressive gain for 28 curing days and 90 curing
20 days with 9.8% and 9.7% respectively.

21 **Keywords**

22 Ball milling, kaolinite, cement, mortar, mechanical performance, pozzolanic reaction.

1 **1. Introduction**

2 Clay minerals are among the most important industrial minerals. Millions of tons are utilized
3 annually in a large variety of applications. These applications include the use in ceramics,
4 papers, plastic, biomedicines, the process industries, agriculture, environmental remediation
5 and construction [1-7]. The name of kaolin is derived from the Chinese term word “Kau-
6 Ling” meaning high ridge, the name of a hill near Jauchau Fu, China, where this material was
7 mined centuries ago for the ceramics manufacturing [1-3]. Kaolin is referred as china clay
8 and contains mainly 85% to 95% of kaolinite. The main kaolinite constituent is a hydrous
9 aluminum silicate of the approximate composition $2\text{H}_2\text{O}\cdot\text{Al}_2\text{O}_3\cdot 2\text{SiO}_2$. In addition to kaolinite,
10 kaolin usually contains quartz and mica and, less frequently, feldspar, illite, montmorillonite,
11 ilmenite, anastase, haematite, bauxite, zircon, rutile, kyanite, silliminate, graphite, attapulgit,
12 and halloysite [1-3]. Kaolin is generally formed by the alteration of Al silicate minerals in a
13 warm and humid environment. It is classified as a two-layer clay, a sheet of tetrahedral silica
14 combined with octagonal hydroxyls, which are shared with alumina octahedral sheet. In the
15 plane of atoms common to both sheets, two thirds are oxygen atoms; one third is composed of
16 hydroxyls. Because of the slight differences in the oxygen-to-oxygen distances in the
17 tetrahedral and octahedral layers, there is some distortion of the ideal tetrahedral network. As
18 a result, kaolinite appears as triclinic instead of being monoclinic. The bonding between
19 successive kaolinite layers is composed of both van Der Waals forces and hydrogen bonds.
20 The bonding is sufficiently strong to prevent interlayer swelling in the presence of water [1-2,
21 7-8]. In different uses and applications of kaolin or kaolinite, researchers are looking for
22 improvement of kaolinite (kaolin) properties by varying the particle size, surface chemistry,
23 particles shape, surface area, and other physical and chemical properties. This improvement
24 depends on the target application. The main searched properties are viscosity, color, plasticity,

1 green, dry and fired strength, absorption and adsorption, abrasion, to cite a few [6, 9-15]. In
2 order to obtain these kaolinite/kaolin properties, several techniques and processes have been
3 proposed such calcination by thermal treatment, alkali-activation, chemical treatment and
4 grinding or milling [6, 16-18]. Calcination of kaolin results in metakaolin, which is
5 considered as a pozzolanic product due to its pozzolanic reaction activation. Several
6 researchers have worked on thermal treatment or calcination of kaolin/kaolinite to formulate
7 new products based on metakaolins or metakaolinites for typical applications such as cement
8 replacement for paste, mortar or concretes [6, 14, 16]. Tironi et al. [16] considered five
9 natural kaolinitic clays from different regions of Argentina, with different kaolinite content,
10 different impurities and different degrees of crystallinity. The authors have performed thermal
11 treatment of these clays with programmable laboratory furnace where samples were heated
12 from the ambient temperature up to 700°C. They found that the compressive strength of
13 blended cements with 30% of calcined clay with medium and high kaolinite contents had
14 reached or surpassed the level of compressive strength of plain Portland cement mortar at 28
15 days [16]. Fernandez et al [14] have calcined different clay minerals such as Kaolinite, illite
16 and montmorillonite at 600°C - 800°C and substituted Portland cement in mortar with 30%.
17 The authors have found that substitution of cement by calcined kaolinite resulted in a
18 considerable increase in the mechanical strength starting from 7 days compared to the control
19 mortar. They have explained this increase by the pozzolanic character of the calcined clay
20 combined with CH in order to form additional C-S-H, filling more space and thus increasing
21 the mechanical properties [14].

22 Grinding is also one of several techniques used for improving kaolinite/kaolin properties.
23 Mechano-synthesis is one these milling techniques used to modify the properties of kaolin or
24 kaolinite [11-12, 15, 17]. Mechano-synthesis is described as a high-energy milling process
25 using balls in which powder particles are subjected to the transfer of mechanical energy to the

1 powder particles by plastic deformation. This mechanical transfer results in the introduction
2 of strain into the powder through generation of dislocations and other defects. These defects
3 act as fast diffusion paths. In addition, refinement of particle size with shape modification and
4 reduction of grain sizes naturally occurs as a consequence of the reduction of the diffusion
5 distances. All these effects lead to distinct structural features that affect the final product and
6 the blended elemental powders during the milling process. Among these properties is the
7 development of a high thermal stable amorphous structure, nanocrystalline and
8 nanocomposite materials that are stable at room temperature. The strong modification in the
9 structure of the processed powder can be understood from the main mechanisms involved
10 during the high-energy ball milling process. Indeed, when the powder mixture is placed in the
11 containers with the balls, the particles composing the powder are subjected to a high-energy
12 collision from the balls. Two main events are witnessed, namely a repeated welding and
13 fracturing of the powder mixture [19-22]. In a previous paper, Hamzaoui et al [12] studied the
14 structural changes related to the mechanical processing of proclay kaolinite. The authors were
15 able to quantify the effect of milling time on the structure and the thermal behavior of proclay
16 kaolinite using planetary ball mills in the friction mode process ($\omega \gg \Omega$). The authors have
17 shown that mechanosynthesis is beneficial to produce amorphous kaolinite without heating or
18 calcination.

19 As a continuous effort to the former work, the objective of this work is to reveal the effect of
20 the milling conditions on the structure and the microstructure of proclay kaolinite. In
21 particular, the potential of milled proclay kaolinite as a component in a modified mortar is
22 demonstrated through the substitution of two different cement grades CEM I and CEM II. The
23 substitution of CEM I, which contains more than 95% of clinker, is targeted to reduce CO₂
24 environmental impact of civil engineering materials. The cement grade CEM II is also used in
25 order to improve the pozzolanic reactions since this grade contains slag (more than 22%).

1 These processes of milled kaolinite are discussed especially from the viewpoint of promoting
2 the mechanical performance of modified mortar under certain percentages of milled kaolinite
3 substitution in cement.

4 **2. Materials and Methods**

5 The cements used in this study are CEM I 52.5 N (cement with $\geq 95\%$ of clinker and $\geq 5\%$ of
6 gypsum and mineral additions) and CEM II/B-M (S-LL) 32.5 R (cement with 62% of clinker,
7 22% of slag and other mineral additions according to EN 197-1 norm) from Ciment Calcia.
8 The kaolinite powder used in this work has a commercial name Proclay kaolinite BR500
9 from Beaujard–Poigny site (France). In order to obtain the chemical composition of proclay
10 kaolinite, elemental analysis is conducted by X-ray fluorescence spectroscopy and carried out
11 using S8 TIGER instrument from Bruker. The chemical composition of the kaolinite obtained
12 using S8 TIGER instrument is given in Table 1.

13 The milling of proclay kaolinite powder is carried out using a planetary high-energy ball mill
14 (Retsch PM 400). This device is composed of four vials mounted on a planar disc. With the
15 rotation of the disc characterized by their speed (Ω), the vials move in a circular and in
16 opposite direction compared to the disc rotation. The vials have a different speed (ω)
17 compared to the discs. The selected rotation speeds of the disc and the vials are $\Omega = 400$ rpm
18 and $\omega = 800$ rpm, respectively. Three milling times t are selected, namely 1 hour, 3 hours and
19 9 hours. Thirty-millimeter diameter steel balls and 500 ml volume steel vials are used. The
20 weight of the powder samples is 260 g per vial. More than 1 kg in total weight is obtained
21 after one milling stage. The ball-to-powder weight ratio is 3.1.

22 We mention that vials of planetary ball mill (RETSCH PM 400) are adequately sealed
23 excluding any risk of air contamination during milling process. Also, in order to avoid iron or
24 chromium contamination of the processed powder by elements from balls or vials, a breather
25 delay of 30 minutes is imposed after 1 hour of milling. This contamination can affect the

1 properties of kaolinite by, for example, leading to the decrease of the specific heat C_p in
2 presence of iron [12]. In fact, the delay of 30 minutes allows the cooling of kaolinite powder
3 that can experience large temperatures, typically between 60°C and 300°C inside the vials
4 especially under long milling time [19-21].

5 X-ray investigations are performed on a Bruker D2 phaser diffractometer using a continuous
6 scanning mode with Cu $K\alpha$ radiation ($\lambda = 0.1541$ nm). The lines are measured in the 2θ range
7 (5–100)° in steps of 0.02° for 10 s. The software used for the evaluation is DIFFRAC.EVA
8 with ICDD PDF2. Preliminary analysis shows that the first half of the 2θ range is the most
9 effective one to determine major structural changes.

10 Particle size distributions are measured with Laser Granulometer (LS 230) allowing for the
11 measurements of particle sizes from 0.04 μm to 2000 μm .

12 The morphology of unmilled and milled powders is characterized using scanning electron
13 microscopy (SEM) equipment (S4800 from Hitachi) with a Bruker energy-dispersive X-ray
14 spectrometry (EDS).

15 The blended cement mortar was prepared using Portland cement (CEM I 52.5 N and CEM
16 II/B-M (S-LL) 32.5 R). The milled kaolinite is added as a substitution material with a varied
17 percentage in the cement (5%, 15%, 30% and 45%). Based on The European Standard EN
18 196-1, each specimen consisted of 450 g of binder (b), 1350 g of standardized sand, 225 mL
19 of water (w). These proportions allow the casting of 40 x 40 x 160 mm mortar bars. The water
20 to binder (w/b) ratio was set to 0.5. The samples were kept for 24 hours and then, the mortar
21 prisms were demolded and submerged in a water bath at 20 °C for 7, 28, and 90 curing days.

22 Mechanical testing is carried out using both MTS 100 KN and 3R 250 KN universal
23 machines. Mechanical characterization corresponds to compression and flexural conditions
24 performed on mortar samples of dimensions 40 x 40 x 160 mm³ at different curing times (7,
25 28 and 90 days). The testing is performed up to the rupture point.

3. Results and discussion

3.1 Characterizations of proclay kaolinite powder

X-ray diffraction patterns of proclay kaolinite powder are shown in Figure 1 for different milling times. The characteristic peaks showing major changes with milling time lie in the range of 5° to 48° . It is observed that, the milling time modifies the color and the structure of proclay kaolinite. The X-ray pattern of the original sample contains two main structures, namely kaolinite and quartz. The peaks relative to quartz are more intense than those of kaolinite. Several researchers report similar structure for various kaolinite minerals [14, 16, 23]. The Kaolinite determined by XRD has a triclinic form, namely kaolinite-1A ($\text{Al}_2\text{Si}_2\text{O}_5(\text{OH})_4$). The kaolinite peaks are detected at 11.89° , 19.85° , 24.87° , 35.1° , 36.2° , 37.9° and 38.7° . These peaks correspond respectively to plans K(001), K(110), K(002), K(130), K(200), K(003) and K(113). The presence of reflection planes K(001) and K(002) close to 11.89° and 24.87° 2θ (Cu $K\alpha$) suggests that kaolinite is not highly ordered in comparison with typical ordered kaolinite reported in the literature [10, 11]. In addition, crystallinity indices can be used as descriptors for featuring different kinds of kaolinites and kaolinite group minerals [24]. Taking as a basis, the measurement of FWHM (Full Width at Half the Maximum) [25], the FWHM for the peaks (001) and (002) are 0.357 and 0.389 respectively. These values show that kaolinite is close to be a disordered structure according to the criteria by Amigo et al [25], where for a disordered kaolinite $\text{FWHM} > 0.4$. The quartz detected in the powder has hexagonal form (P3221). The quartz peaks are detected at 20.9° , 26.6° , 36.6° , 39.5° , 40.3° , 42.5° and 45.8° , and these correspond to plans Q(100), Q(101), Q(110), Q(102), Q(111), Q(200) and Q(201) respectively. After milling, it is observed that the characteristic kaolinite lines mostly decrease after one hour of milling. Kaolinite peaks disappear as the result of the deterioration of the kaolinite structure. The milling process induces dihydroxylation and the consequential transformation of kaolinite leads to a very

1 disordered (amorphous) structure (Fig. 1). This structural modification at the atomic scale is
2 concomitant with the change in particle size and morphology observed by other means such
3 as SEM. This result demonstrates that, during milling process, the kaolinite phase becomes
4 gradually distorted and amorphous. After three hours of milling, the XRD pattern reflects the
5 completion of kaolinite amorphous structure formation with the presence of nanocrystalline
6 quartz. More details concerning the discussion of kaolinite structure evolution is available in
7 [12].

8 A similar result about the milling process was found by Miyazaki et al. [15], where UF mill
9 was used to grind kaolinite at different milling times. These products were analyzed by XRD
10 and results obtained are similar to the ones achieved in this study. In addition, the authors [15]
11 have found that after four hours of ball milling, a very large part of kaolinite is found
12 amorphized. The same results was obtained by Dellisanti & Valdre [18] by using a planetary
13 mill for 20 hours. The authors have found that kaolinite peaks were reduced and evidence of
14 kaolinite amorphization was observed. The effect of high energy ball milling on the quartz is
15 not strong enough (Fig. 1). The intensity of the quartz peaks does not decrease in a significant
16 way. However, the peak broadening is observed as in the case of the plans Q(001) and
17 Q(101). For the unmilled kaolinite, the bounded peak Q(001) lies between 20.66° and 21.19° .
18 After 9 hours of milling, this same peak is shifted between 20.69° and 21.40° . In a similar
19 way, the peak Q(101) in the range 26.39° to 26.97° is identified for the unmilled kaolinite.
20 This peak is shifted backwards to the range (26.26° - 27.28°) after 9hours of milling. The
21 broadening of the quartz peaks is observed with a slight intensity reduction, meaning that the
22 reduction of crystallites size of the quartz is achieved.

23 To better understand the mesostructural modifications obtained by mechanosynthesis for
24 different milling times, laser granulometry results are used to interpret particle size

1 distribution (figure 2) and SEM micrographs are exploited to analyze the particle morphology
2 modifications (Figure 3).

3 The effect of high energy ball milling on the quartz was not strong enough (Fig. 1). The
4 intensity of the quartz peaks did not decrease. However, peak broadening is observed, which
5 means that the reduction of crystallites size of the quartz is achieved.

6 Particle size distribution of kaolinite is shown in Figure 2a as function milling time. It is
7 observed that the unmilled kaolinite has a multimodal distribution, which is clearly evidenced
8 on a logarithmic scale. Four distinct meaningful particle size ranges are observed. The first
9 one corresponds to a small particle population with typical sizes between 0.37 μm and 3 μm
10 and a maximum peak found at 2.1 μm . The second range between 3 μm and 17.5 μm
11 concerns slightly larger particles with a peak at 11.6 μm . The third range is an intermediate
12 one and refers to particle sizes from 17.5 μm to 40 μm and with peak position at 29.9 μm . The
13 largest particle population has a typical size between 40 μm and 100 μm with a peak recorded
14 at 67.9 μm . Generally speaking, particle size distributions of kaolinite or kaolin are reported
15 to have modal, bimodal and multimodal distribution [4, 13, 18, 26-29]. For instance, the
16 Vizcaino et al. [26] achieved both bimodal and multimodal distributions upon physical-
17 chemical alterations by mechanochemical treatments of two natural kaolinites.

18 For untreated kaolinite, Melo et al. [28] have found that kaolinite forms a very cohesive
19 material and forming micronize agglomerates. Makó et al. [29] have found that particles of
20 natural kaolinite from Bringwood are mostly below 0.5 μm , and form stacks, individual fine
21 thin plates. These plates have a pseudo-hexagonal shape but most of them are fairly ragged.

22 There is an overall consensus in the literature that kaolinite exhibit a relatively sharp
23 crystalline morphology with a pseudo-hexagonal shape [7, 11, 27-30].

24 Concerning the effect of milling time, it has been observed that after one hour of milling,
25 kaolinite granulometry transforms to a bimodal distribution where the size of the first particle

1 population varies between 0.4 μm to 17.7 μm with a peak around 11.7 μm . The second
2 particle population has a typical size between 17.7 μm and 100 μm with maximum value at
3 33.1 μm . It can be deduced that after one hour of milling, the first particle population can be
4 considered as a result of particle fracturing among the third and fourth population of the
5 particles in the unmilled kaolinite. It can be also deduced that the largest particles in the
6 milled powder results from the agglomeration events of the largest population in the unmilled
7 powder. In addition, agglomeration can also take place within the three smallest particle
8 populations in the unmilled powder to form the largest particles in the milled powder. Also, the
9 two largest particle populations in the unmilled powder can lead to the smallest population in
10 the milled powder.

11 Concerning kaolinite milled 3h and 9h, a multimodal distribution is observed, which is
12 characterized by three peaks. For kaolinite milled at 3h, the first peak at 1.9 μm is found
13 between 0.34 μm to 3.5 μm . the second peak of 10 μm concerns a particle population with a
14 size between 3.5 μm to 15 μm . The third population lies within a size interval between 15 μm
15 and 64 μm with peak position at 40 μm . For the milled kaolinite at 9h, the first particle size
16 range is situated between 0.34 μm to 4.2 μm with maximum at 1.8 μm . The second range is
17 positioned between 4.2 μm and 16.5 μm with a peak at 9.9 μm . The third range is limited
18 between 16.5 μm and 59 μm with peak position at 41 μm . The comparison between unmilled
19 and milled kaolinite leads to the general observation of the reduction of large particles from
20 100 μm to 64 and 59 μm after 3h and 9h of milling, respectively. Also, the first and second
21 particle populations of unmilled kaolinite overlap with the smallest particles for both milled
22 kaolinite at 3h and 9h. This result shows that the milling process affects more the large
23 particles than the small ones. Dellisanti & Valdre [18] observed that after 1h of milling of an
24 industrial kaolin that exhibited a modal particle size distribution, the particle size distribution
25 did not vary. They observed a significant modification of the particle size distribution, which

1 became a bimodal distribution after 5 hours of milling. The two maxima of the bimodal
2 distribution were centered at about 5 μ m and 50 μ m. In addition, the authors remarked that the
3 milling performed to longer times (10h and 20h) had led to a modal distribution with larger
4 particle sizes compared to 2.3 μ m of the original distribution. The peak positions for the final
5 distributions reached at of 78 μ m and 100 μ m, for 10h and 20h of milling, respectively.

6 In order to complete the analysis of the particle size distribution, Figure 2b presents the
7 variation of the medium particle size D50% based on the cumulative form of the size
8 distribution shown in Figure 2a. It can be seen that the ball milling has an overall effect of
9 particle size reduction. Also, it can be observed that the distribution of untreated kaolinite has
10 the largest particles. After ball milling, the particle size decreases as a function of milling time
11 up to 9 hours.

12 Figure 2c shows the evolution of the average particle size D50% of the kaolinite as a function
13 of the milling time [12]. This quantity is reduced from 13.0 μ m for the untreated proclay to
14 8.9 μ m for proclay kaolinite after 9 hours of ball milling. From overall trend of D50%, it can
15 be stated that the grinding is more effective after 1 h of milling time. After 3 hours of ball
16 milling, the particle size reaches 9.8 μ m and the rate of particle size reduction is less efficient
17 for 9h of ball milling. Using planetary ball mill, Koç et al. [27] have found that unmilled
18 Kaolinite are composed of individual platelets that agglomerate into larger particles. After 1 h
19 of mechanical activation, the particle size was less than 3 μ m. However, the authors have
20 found that after 2 h of milling, the particles were agglomerated. In addition, the authors have
21 found that D50% decreased from 6.7 μ m to 4.8 μ m within 2 h of milling. Using planetary ball
22 mill (Fritsch P6) for milling the mixture of natural kaolinite for different milling times,
23 Sahnoune et al. [30] have shown that unmilled kaolinite have irregular shapes and large
24 particle size distribution. However, milling for 5 h decreased the particle size, and yielded a
25 homogeneous powder mixture with particles having almost spherical shape. In addition, Makó

1 et al [29] have shown that, after 2 h of grinding, the primary particle size is strongly reduced
2 and the original particle shape of kaolinite is ruined forming compact agglomerates.
3 Figure 3 exhibits SEM micrographs of the kaolinite at different milling times. Figure 3a
4 shows the powder morphology of the raw kaolinite. At this initial stage, the particles mostly
5 form stacks and flat particles with irregular shapes. In addition, different particle sizes can be
6 distinguished, which explains the presence of a multimodal particles distribution with four
7 typical populations. After 1h of milling (Figure 3b), the breaking of some plate particles is
8 observed with slight particle size reduction and change to spherical shape. In addition, it
9 remarked that agglomeration phenomena of thin particles take place, which certainly explain
10 the evolution of the particle size distribution from multimodal with 4 particle size ranges to a
11 bimodal distribution. For the milling times of 3 h and 9h (Figure 3c, 3d), a significant particle
12 size reduction is observed. There is a total disappearance of the plate particles and the final
13 particle morphology appears irregular, especially after 9h of milling [12]. In addition, the
14 phenomena of agglomeration of thin particles are predominant and leads to the presence of
15 opaque zones. In mechanosynthesis, particle size reduction, shape changes and particles
16 agglomeration are typical phenomena that originate from the movement of fracturing and
17 welding and lead to the shock and trapping of powders between balls or between the balls and
18 the vial walls [19-22].

19 **3.2 Cement substitution with milled proclay kaolinite**

20 The results of compression strength tests on the substituted mortar prepared with CEM I and
21 CEM II are presented in Figure 4. The reference mortar prepared with CEM I without
22 substitution exhibits a compression strength of 38.5, 48.0 and 49.9 MPa after 7, 28 and 90
23 days, respectively. For the reference mortar prepared with CEM II without substitution the
24 compression strength are 30.7, 36.7, and 39.2 MPa for 7, 28 and 90 days, respectively.
25 Concerning the modified mortars based on CEM I, it is observed that the substitution with

1 unmilled kaolinite decreases dramatically the compressive strength especially for 30% and
2 45% (Figure 4a) where, for 45% of substitution at 7 curing days, the compression strength is
3 impossible to determine because of lack of mechanical stability. The large decreasing trend in
4 compression strength reaches 87% with respect to the reference mortar for 45% of
5 substitution with unmilled kaolinite at 28 curing days. This result is in qualitative agreement
6 with the reported trend by He et al. [31], which demonstrates the decrease of the compression
7 strength of mortars modified by untreated kaolinite. It is noticed that the substitution of
8 unmilled kaolinite directly affects the workability of modified mortar because kaolinite has a
9 higher sensitivity to water absorption. An opposite trend is observed for mortars substituted
10 with milled kaolinite. For all attempted milling times (1h, 3h, and 9h) and all substitution
11 rates (5%, 15%, 30% and 45%), the compression strength of these modified mortars is
12 superior to the one of mortars modified with unmilled kaolinite. The best performing
13 formulation refers to a substitution with 15% of milled kaolinite and a milling time of 9 h. In
14 this case, the gain in compression strength reaches 18.9% and 25.0% after 28 and 90 days,
15 respectively. For all mortars made with kaolinite milling, an important gain in compressive
16 strength is observed between 7 and 28 days, due to the effect of the pozzolanic reaction.

17 Concerning the mortars prepared using CEM II grade, the results shown in Figure 4b suggest
18 the same decreasing trend in the compression strength that culminates at 71.9% of loss in
19 performance for 45% of substitution with unmilled kaolinite at 90 curing days. However,
20 mortars substituted with milled kaolinite all exhibit gain in compression strength irrespective
21 of amount of substitution and milling time.

22 When compared to the reference mortar, the best performing mortar is the one formulated
23 with 15% of kaolinite milled during 9 h. Indeed, the gain in compression strength for this
24 mortar reaches 10.0% and 9.7% after 28 and 90 curing days, respectively.

1 Fernandez et al [14] have studied the effect of calcined clays at high temperatures (600 °C and
2 800 °C) on cement formulation. In particular, the authors compared the behavior of calcined
3 kaolinite, illite and montmorillonite considered as substitutes to CEM I by an amount of 30%.
4 The authors found that calcined illite and calcined montmorillonite decreased dramatically the
5 compression strength of formulated mortars. However, calcined kaolinite at 600°C increased
6 the compression strength of the modified mortars by 18%, 10% and 3% for 7, 28 and 90
7 curing days, respectively. The authors explained the gain in mechanical performance by the
8 pozzolanic character of the calcined kaolinite. Also, Tironi et al [16] studied cement
9 replacement by 30% of two calcined kaolinite from Argentina at 700°C. The authors have
10 shown that one of the calcined kaolinite improved the compression strength of mortar by
11 28%. The literature analysis shows that calcined kaolinite, metakaolinite and
12 nanometakaolinite increase the compression strength of mortars and pastes with substituted
13 cement from 5% to 30% depending on the reported works [14, 16, 23, 31-33].
14 Figure 5 shows the flexural strength of all formulated mortars as function of curing days. The
15 flexural strength of the reference mortar formulated with CEM I shows a slight increasing
16 trend from 7.5 MPa to 8.2 MPa between 7 and 90 curing days (Figure 5a). The same slight
17 improvement of the flexural strength is achieved for the reference mortar prepared with CEM
18 II. This increase in flexural strength goes from 7.0 MPa to 8.3 MPa between 7 and 90 curing
19 days. The CEM I substitution by unmilled kaolinite has a negative effect on the flexural
20 strength especially for formulation with 30% and 45% of cement substitution (Fig. 5a). The
21 largest loss in performance is estimated at 68.8% compared to the reference mortar for 45% of
22 cement substitution with unmilled kaolinite at 28 curing days. In the opposite case, mortars
23 substituted with milled kaolinite all exhibit flexural strengths greater than the ones prepared
24 with unmilled kaolinite. Among the modified mortars, those prepared with milled kaolinite
25 during 3h and 15% of substitution have a flexural performance close to the one of the

1 reference mortar. The best performing one allows a flexural strength gain of 12.1% after 28
2 curing days. Concerning the mortars prepared with CEM II, a similar behavior is obtained
3 (Figure 5b). Unmilled kaolinite is found to have a negative effect on the flexural strength and
4 milled kaolinite is found to have the opposite effect.

5 Replacing cement with nanometakaolin from 5% to 15% by weight, Morsy et al. [33] found
6 that the gain in both compression and flexural strength of modified mortars is only achieved
7 for a replacement by 5%. The replacement of cement by nanometakaolin enhances the
8 compression and flexural strengths up to 15% by weight.

9 Based on the result of XRD patterns (Figure 1), the observed gain in mechanical strength for
10 the formulations with milled kaolinite is attributed to the deterioration of the kaolinite original
11 structure and the formation of a very disordered amorphous medium. But it seems that 3 hours
12 of milling for which the completion of kaolinite structure formation is observed, are not
13 enough to obtain the largest mechanical performance. These are related to larger milling times
14 of the order of 9 hours. In fact, the results of particle size distribution help to explain the need
15 for a larger milling time (Figure 2), as it is observed a shift from a bimodal to multi-modal
16 size distributions when milling time is increased from the small (1h to 3 h) to the large (3h to
17 9 h). Thus the need for a larger milling time can be justified by the combination of kaolinite
18 complete amorphisation and a wide dispersion in granulometry. Also, at large milling times,
19 the agglomeration of particles and the formation of a more irregular particle morphology help
20 to increase the surface area (Figure 3). This last argument corroborates the optimal
21 performance achieved for large milling times. Based on the results of the mechanical testing
22 of modified mortars, the optimal formulations seem to privilege the 15% as an amount of
23 substitution. In the following, this study focuses on the formulations considered with this
24 amount of substitution.

1 In order to understand the thermal behavior of modified mortars with 15% of kaolinite, DSC
2 analysis is undertaken within the temperature range (25–550) °C as shown in Figure 6. It is
3 worth mentioning that assessment of the weight loss above 900°C is recommended to verify
4 the carbonation phenomena. However, the DSC machine available for this study can only
5 reach 600°C. For both cement grades, there are two endothermic regions of major hydraulic
6 products associated with the decomposition of both adsorbed and crystalized water. The first
7 region positioned at 100–225°C, which refers to the combination of two peaks located at
8 about 100°C- 175°C and 175°C- 225°C. It is widely admitted that the first peak is attributed
9 to the decomposition of the calcium silicate hydrates (C-S-H), the calcium sulpho-aluminate
10 hydrates (ettringite) [34-37] whereas the second peak corresponds to monosulfate (Afm), C-S-
11 H, calcium aluminate hydrates (C-A-H) and calcium aluminate silicate hydrate (C-A-S-H)
12 [37-39]. In the present case, it is suggested that the region located at 100°C-225°C includes
13 two peaks, and these correspond to the decomposition of C-S-H, ettringite, Afm and C-A-H
14 without any distinction. The second region locates an endothermic peak, which is observed
15 between 450°C and 525 °C. This peak represents the decomposition of the portlandite Ca
16 (OH)₂.

17 To follow the enthalpy change (ΔH) associated with the decomposition of both adsorbed and
18 crystalized water, an estimate on the areas under the endothermic peaks in the temperature
19 ranges (100 – 175)°C, (175 – 225)°C and (450 – 525)°C is provided. Table 2 summarizes
20 (ΔH) values for mortars modified with 15% of milled kaolinite at 90 curing days as a function
21 of milling time. Within the temperature ranges (100 – 175) °C and (450 – 525) °C, ΔH values
22 associated with the reference mortar (RMCI and RMCII) are similar to the ones of mortars
23 prepared with natural kaolinite (NKCI and NKCI). Only minor differences are observed for
24 the first peak ranges in the temperature (100 – 175) °C (Figure 6, Table 1). The second peak
25 identified in the temperature range (450 – 525)°C for the reference mortar is larger compared

1 to formulations with natural kaolinite. The mortar based on CEM I grade and prepared with
 2 kaolinite milled for 1h has the same behavior than the reference mortar. By opposition, the
 3 mortar prepared with CEM II using the same substitution exhibits a reduction of the
 4 portlandite peak by 37.2% and an increase of ΔH peaks within the region (100 – 225) °C
 5 estimated to 42.5% in comparison with the reference mortar. Mortars prepared with milled
 6 kaolinite during larger times (> 1 h) exhibit the same changing behavior, irrespective of the
 7 cement grade. Indeed, it is found that the portlandite peak decreases by 65.8% and 64.0%
 8 compared to the reference CEM I mortar for mortars prepared with kaolinite milled for 3h and
 9 9h, respectively. The same decreasing trend by 58.9% and 61.4 of the portlandite peak is
 10 found for CEM II mortars prepared with the same kaolinite milling conditions.

11 In addition, in the temperature range (100 – 225)°C, the two identified peaks are higher for
 12 mortars prepared with kaolinite milled for 3h and 9h than the ones of the reference mortars
 13 based on CEM I and CEM II grades. The increase in peak height is estimated to 36.1% and
 14 33.2% for CEM I at 3h and 9h of milling and 38.7%, 42.7% for CEM II at 3h and 9h of
 15 milling, respectively. The increasing trend of the two peaks in temperature range (100 –
 16 225)°C and the decaying portlandite peaks can be attributed to the pozzolanic reactions
 17 between the activated milled kaolinite and the calcium hydroxide in both CEM I and CEM II
 18 cements. The hydration process of Portland cement can be summarized as follows [39-40]:



21 Whereas the pozzolanic reaction can be summarized as flows [41]:



24 Where C: CaO, S: SiO₂, A: Al₂O₃, H: H₂O, CH: Ca (OH)₂.

1 From the expressions (3) and (4), the active silica (SiO_2) and aluminate (Al_2O_3) of milled
2 kaolinite react with calcium hydroxide originated from Portland cement hydration giving rise
3 to calcium silicate hydrate, i.e., C-S-H like in expression (3) or calcium aluminate hydrate,
4 i.e., C-A-H like in expression (4). The formation of secondary C-S-H by pozzolanic reactions
5 in mortar with milled kaolinite contributes to the improvement of the mechanical performance
6 of modified mortar. Thus, it can be said that the remarkable effect of high-energy milling on
7 the mechanical performance of modified mortars can be understood as an activation of
8 kaolinite and the development of pozzolanic reactions. .

9 **3 Conclusions**

10 In this work, the study of the ball milling of kaolinite powders at different milling times from
11 the structural, mechanical and thermal point of views allows the following conclusions:

12 1) X-ray patterns indicate that characteristic proclay kaolinite lines decrease gradually in
13 intensity. After 3 h of milling, kaolinite amorphous structure is obtained. Quartz with
14 hexagonal structure is characterized by nanocrystallite size after milling. Regarding the size
15 distribution of the different kaolinite milled powders, it can be concluded that the milled
16 kaolinite at 9h has the lowest particle size distribution.

17 2) Substitution of CEM I and CEM II by natural kaolinite dramatically decrease the
18 mechanical strength. After a curing time of 7 days, the substitution with 45% of natural
19 kaolinite leads even to mechanical instability. Substitution of CEM I and CEM II milled
20 kaolinite in modified mortar allows a substantial improvement of the compression strength.
21 As early as 7 days of curing, the modified CEM I and CEM II mortars reach the compression
22 strength of the reference mortars with only 5% of kaolinite substitution milled to durations
23 larger than 1 hour. The best compression strength gain for 15% of milled kaolinite after 9h of
24 milling. The highest gain compression strength is measured as 25% in the case of CEM I for
25 90 curing days and 10% for CEM II after 28 curing days. This high gain can be attributed to

1 the complete amorphisation of kaolinite due to the high energy of milling. This amorphisation
2 allows the pozzolanic reaction activation and the formation of secondary CSH from
3 portlandite and silicates.

4 3) The DSC results revealed the significance of the pozzolanic reactions, which can be
5 summarized as a decreasing trend in the decomposition enthalpy of portlandite for milled
6 kaolinite-based mortars compared to the reference mortar. This trend is the result of
7 portlandite consumption in the pozzolanic reactions by milled kaolinite.

8 4) High energy milling can be considered as beneficial for the activation of both kaolinite
9 and pozzolanic reactions. However, 3h and 9h of milling times are too large. Such milling
10 times require large energy consumption in comparison with the methods used to obtain
11 metakaolinite. From an industrial point of view, it will be suitable to optimize the milling
12 conditions to reduce the milling time between 5 and 15 minutes.

13 **Acknowledgments**

14 The authors are grateful to Marc Bonnet from ENS Cachan for technical assistance with SEM
15 analysis and to Margareta Walferdein from ESTP Cachan for her technical assistance with
16 mechanical and thermal tests.

17

References

[1] Z. Adamis, J. Fodor, R.B. Williams, Environmental health criteria 231: Bentonite, kaolin,
and selected clay minerals, WHO Geneva, 2005. doi:10.1016/0043-1354(85)90052-1.[2] [1]

H.. Murray, Applied clay mineralogy today and tomorrow, Clay Miner. 34 (1999) 39–49.
doi:10.1180/000985599546055.

[3] A.J. Bloodworth, D. E. Highley, C. J. Mitchell, Industrial Minerals laboratory Manual,
Technical report WG/93/1, Mineralogy and petrology series, ODA, British geological survey,
1993, 1-76

- [4] J.-F. Zhang, Q.-H. Zhang, J.P.-Y. Maa, Coagulation processes of kaolinite and montmorillonite in calm, saline water, *Estuar. Coast. Shelf Sci.* 202 (2018) 18–29. doi:10.1016/J.ECSS.2017.12.002.
- [5] J. Yuan, J. Yang, H. Ma, S. Su, Q. Chang, S. Komarneni, Hydrothermal synthesis of nano-kaolinite from K-feldspar, *Ceram. Int.* 44 (2018) 15611–15617. doi:10.1016/J.CERAMINT.2018.05.227..
- [6] R. Siddique, J. Klaus, Influence of metakaolin on the properties of mortar and concrete: A review, *Appl. Clay Sci.* 43 (2009) 392–400. doi:10.1016/J.CLAY.2008.11.007.
- [7] M.E. Awad, A. López-Galindo, M. Setti, M.M. El-Rahmany, C.V. Iborra, Kaolinite in pharmaceuticals and biomedicine, *Int. J. Pharm.* 533 (2017) 34–48. doi:10.1016/J.IJPHARM.2017.09.056..
- [8] A. Meunier, Crystal Structure — Species — Crystallisation, in: *Clays*, Springer-Verlag, Berlin/Heidelberg, 2005: pp. 1–60. doi:10.1007/3-540-27141-4_1..
- [9] J.-E. Otterstedt, D.A. Brandreth, Clays and Colloidal Silicas, in: *Small Part. Technol.*, Springer US, Boston, MA, 1998: pp. 155–183. doi:10.1007/978-1-4757-6523-6_4.
- [10] [1] M. Valášková, K. Barabaszová, M. Hundáková, M. Ritz, E. Plevová, Effects of brief milling and acid treatment on two ordered and disordered kaolinite structures, *Appl. Clay Sci.* 54 (2011) 70–76. doi:10.1016/J.CLAY.2011.07.014..
- [11] M. Valášková, K. Barabaszová, M. Hundáková, M. Ritz, E. Plevová, Effects of brief milling and acid treatment on two ordered and disordered kaolinite structures, *Appl. Clay Sci.* 54 (2011) 70–76. doi:10.1016/J.CLAY.2011.07.014.

- [12] R. Hamzaoui, F. Muslim, S. Guessasma, A. Bennabi, J. Guillin, Structural and thermal behavior of proclay kaolinite using high energy ball milling process, *Powder Technol.* 271 (2015) 228–237. doi:10.1016/j.powtec.2014.11.018..
- [13] M. Hassellöv, B. Lyvén, H. Bengtsson, R. Jansen, D.R. Turner, R. Beckett, Particle size distributions of clay-rich sediments and pure clay minerals: A comparison of grain size analysis with sedimentation field-flow fractionation, *Aquat. Geochemistry.* 7 (2001) 155–171. doi:10.1023/A:1017905822612.
- [14] R. Fernandez, F. Martirena, K.L. Scrivener, The origin of the pozzolanic activity of calcined clay minerals: A comparison between kaolinite, illite and montmorillonite, *Cem. Concr. Res.* 41 (2011) 113–122. doi:10.1016/j.cemconres.2010.09.013.
- [15] M. Miyazaki, M. Kamitani, T. Nagai, J. Kano, F. Saito, Amorphization of kaolinite and media motion in grinding by a double rotating cylinders mill - a comparison with a tumbling ball mill, *Adv. Powder Technol.* 11 (2000) 235–244. doi:10.1163/156855200750172349.
- [16] A. Tironi, M.A. Trezza, A.N. Scian, E.F. Irassar, Kaolinitic calcined clays: Factors affecting its performance as pozzolans, *Constr. Build. Mater.* 28 (2012) 276–281. doi:10.1016/j.conbuildmat.2011.08.064.
- [17] R.L. Frost, J. Kristóf, É. Makó, E. Horváth, A DRIFT spectroscopic study of potassium acetate intercalated mechanochemically activated kaolinite, *Spectrochim. Acta - Part A Mol. Biomol. Spectrosc.* 59 (2003) 1183–1194. doi:10.1016/S1386-1425(02)00317-7.
- [18] F. Dellisanti, G. Valdrè, The role of microstrain on the thermostructural behaviour of industrial kaolin deformed by ball milling at low mechanical load, *Int. J. Miner. Process.* 102–103 (2012) 69–77. doi:10.1016/j.minpro.2011.09.011.

- [19] C. Suryanarayana, Mechanical alloying and milling, *Prog. Mater. Sci.* 46 (2001) 1–184. doi:10.1016/S0079-6425(99)00010-9.
- [20] M.S. El-Eskandarany, Mechanical Alloying for Fabrication of Advanced ENGINEERING MATERIALS, WILLIAM ANDREW PUBLISHING, 2001. doi:10.1016/B978-0-8155-1462-6.50012-3. .
- [21] E. Gaffet, G. Le Caër, Mechanical Processing for Nanomaterials, in: H.S. Nalwa (Ed.), *Encycl. Nanosci. Nanotechnol.*, American Scientific Publishers, 2004: pp. 91–129. *Mechanical_Processing_for_Nanomaterials*.
- [22] R. Hamzaoui, O. Elkedim, N. Fenineche, E. Gaffet, J. Craven, Structure and magnetic properties of nanocrystalline mechanically alloyed Fe-10% Ni and Fe-20% Ni, *Mater. Sci. Eng. A.* 360 (2003) 299–305. doi:10.1016/S0921-5093(03)00460-X.
- [23] B. Samet, T. Mnif, M. Chaabouni, Use of a kaolinitic clay as a pozzolanic material for cements: Formulation of blended cement, *Cem. Concr. Compos.* 29 (2007) 741–749. doi:10.1016/j.cemconcomp.2007.04.012.
- [24] P. Aparicio and E. Galan, Mineralogical interference on kaolinite crystallinity index measurements, *Clays and Clay Minerals.* 47 (1999) 12-27.
- [25] J.M. Amigo, J. Bastida, A. Sanz, M. Signes, J. Serrano, Crystallinity of Lower Cretaceous kaolinites of Teruel (Spain), *Applied Clay Science* 9 (1994) 51-69.
- [26] C. Vizcayno, R. Castelló, I. Ranz, B. Calvo, Some physico-chemical alterations caused by mechanochemical treatments in kaolinites of different structural order, *Thermochim. Acta.* 428 (2005) 173–183. doi:10.1016/j.tca.2004.11.012.

- [27] S. Koç, N. Toplan, K. Yildiz, H.Ö. Toplan, Effects of mechanical activation on the non-isothermal kinetics of mullite formation from kaolinite, *J. Therm. Anal. Calorim.* 103 (2011) 791–796. doi:10.1007/s10973-010-1154-5.
- [28] J.D.D. Melo, T.C. de Carvalho Costa, A.M. de Medeiros, C.A. Paskocimas, Effects of thermal and chemical treatments on physical properties of kaolinite, *Ceram. Int.* 36 (2010) 33–38. doi:10.1016/j.ceramint.2009.06.017.
- [29] É. Makó, J. Kristóf, E. Horváth, V. Vágvölgyi, Mechanochemical intercalation of low reactivity kaolinite, *Appl. Clay Sci.* 83–84 (2013) 24–31. doi:10.1016/j.clay.2013.08.002. .
- [30] F. Sahnoune, M. Chegaar, N. Saheb, P. Goeuriot, F. Valdivieso, Algerian kaolinite used for mullite formation, *Appl. Clay Sci.* 38 (2008) 304–310. doi:10.1016/j.clay.2007.04.013..
- [31] C. He, B. Osbaeck, E. Makovicky, Pozzolanic reactions of six principal clay minerals: Activation, reactivity assessments and technological effects, *Cem. Concr. Res.* 25 (1995) 1691–1702. doi:10.1016/0008-8846(95)00165-4.
- [32] M. Said-Mansour, E.-H. Kadri, S. Kenai, M. Ghrici, R. Bennaceur, Influence of calcined kaolin on mortar properties, *Constr. Build. Mater.* 25 (2011) 2275–2282. doi:10.1016/J.CONBUILDMAT.2010.11.017. .
- [33] M.S. Morsy, Y.A. Al-Salloum, H. Abbas, S.H. Alsayed, Behavior of blended cement mortars containing nano-metakaolin at elevated temperatures, *Constr. Build. Mater.* 35 (2012) 900–905. doi:10.1016/j.conbuildmat.2012.04.099.
- [34] S.M.A. El-Gamal, M.S. Amin, M. Ramadan, Hydration characteristics and compressive strength of hardened cement pastes containing nano-metakaolin, *HBRC J.* 13 (2017) 114–121. doi:10.1016/j.hbrcj.2014.11.008.

- [35] E. Benhelal, M.I. Rashid, C. Holt, M.S. Rayson, G. Brent, J.M. Hook, M. Stockenhuber, E.M. Kennedy, The utilisation of feed and byproducts of mineral carbonation processes as pozzolanic cement replacements, *J. Clean. Prod.* 186 (2018) 499–513. doi:10.1016/J.JCLEPRO.2018.03.076. .
- [36] X. Zhang, Y. He, C. Lu, Z. Huang, Effects of sodium gluconate on early hydration and mortar performance of Portland cement-calcium aluminate cement-anhydrite binder, *Constr. Build. Mater.* 157 (2017) 1065–1073. doi:10.1016/J.CONBUILDMAT.2017.09.153.
- [37] X. Lu, Z. Ye, L. Zhang, P. Hou, X. Cheng, The influence of ethanol-diisopropanolamine on the hydration and mechanical properties of Portland cement, *Constr. Build. Mater.* 135 (2017) 484–489. doi:10.1016/J.CONBUILDMAT.2016.12.191. .
- [38] Y. Liu, S. Lei, M. Lin, Z. Xia, Z. Pei, B. Li, Influence of calcined coal-series kaolin fineness on properties of cement paste and mortar, *Constr. Build. Mater.* 171 (2018) 558–565. doi:10.1016/J.CONBUILDMAT.2018.03.117.
- [39] E.G. Nawy, *Concrete Construction Engineering Handbook*, CRC Press, 2008. doi:10.1152/ajpendo.00206.2015.
- [40] A. Bouaziz, R. Hamzaoui, S. Guessasma, R. Lakhal, D. Achoura, N. Leklou, Efficiency of high energy over conventional milling of granulated blast furnace slag powder to improve mechanical performance of slag cement paste, *Powder Technol.* 308 (2017) 37–46. doi:10.1016/j.powtec.2016.12.014.
- [41] Q. Zeng, K. Li, T. Fen-Chong, P. Dangla, Determination of cement hydration and pozzolanic reaction extents for fly-ash cement pastes, *Constr. Build. Mater.* 27 (2012) 560–569. doi:10.1016/j.conbuildmat.2011.07.007.

Figure captions

Fig. 1. X-ray diffraction patterns of kaolinite samples after different mechanical milling times (0h, 1h, 3h, and 9h).

Fig.2. Particle size distribution analysis of kaolinite at different milling times (0h, 1h, 3h and 9h). (a) Size distribution, (b) Median particle size D50%.

Fig. 3. SEM images of kaolinite at different milling stages: (a) Raw, (b) 1 h, (c) 3h, (d) 9 h.

Fig. 4 The evolution of compressive strength (a) CEM I, (b) CEM II as function of substitution rate for mortars.

Fig. 5 The evolution of flexural strength (a) CEM I, (b) CEM II as function of substitution rate for mortars.

Fig. 6. DSC curves of hardened mortars at 90 days. (a) 15% kaolinite+ 85% CEM I, (b) 15% kaolinite+ 85% CEM II.

List of tables

Table.1 Chemical composition of proclay kaolinite powder.

Table. 2 Decomposition enthalpy of C-A-H, C-S-H and Ca(OH)_2 of substituted (CEM I, CEM II) mortars with 15% of kaolinite at 90 curing days.

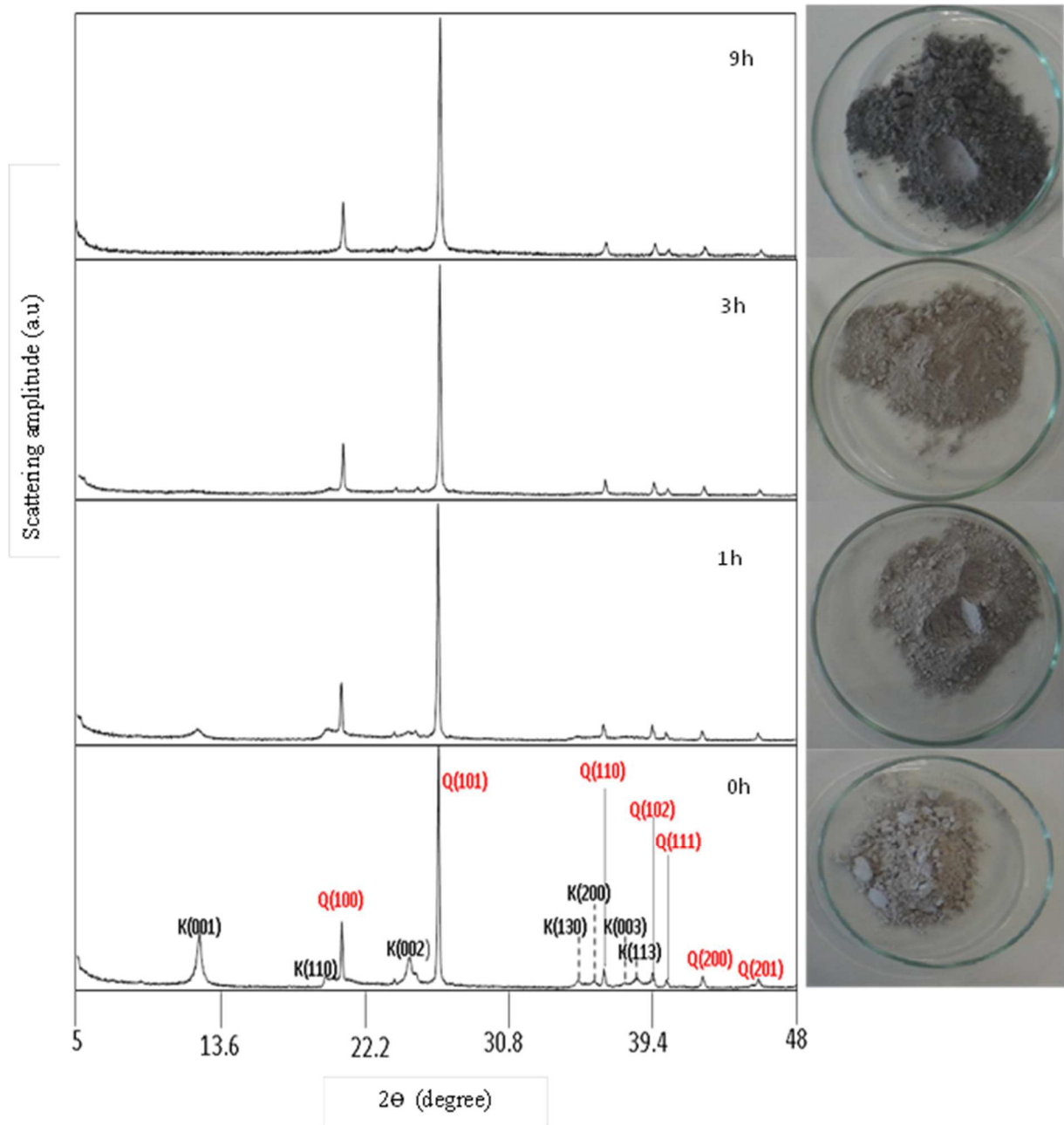
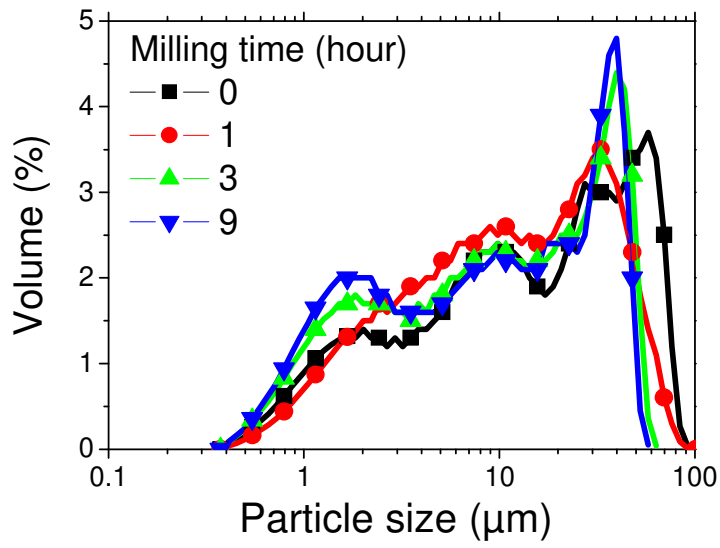
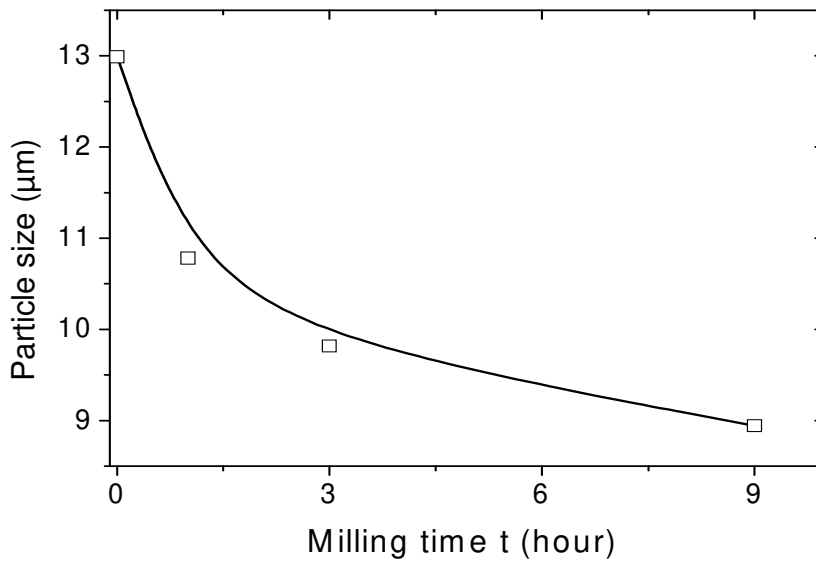


Fig. 1. X-ray diffraction patterns of kaolinite samples after different mechanical milling times (0h, 1h, 3h, and 9h).

1

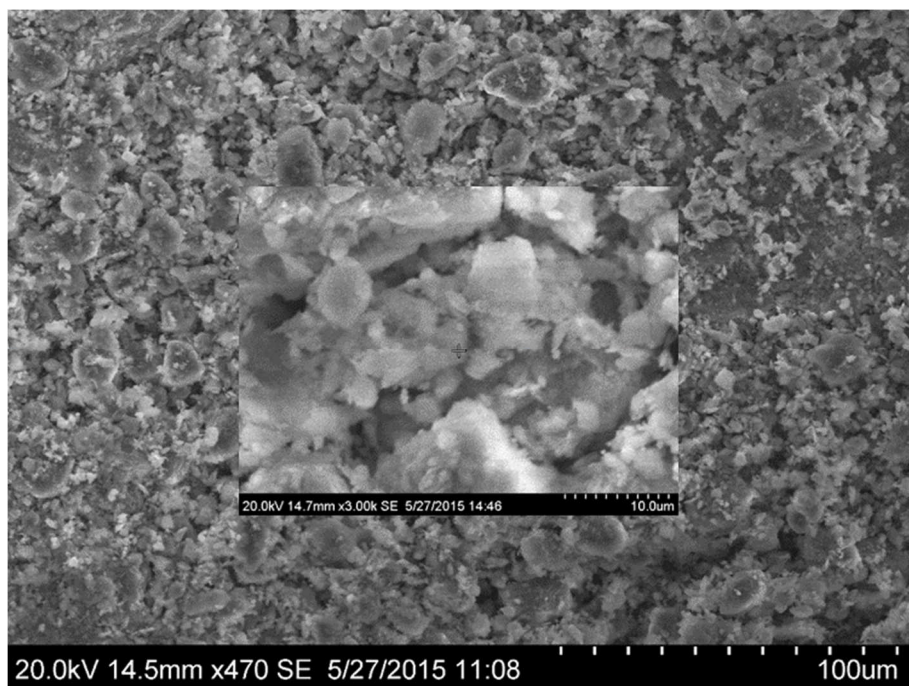


(a)

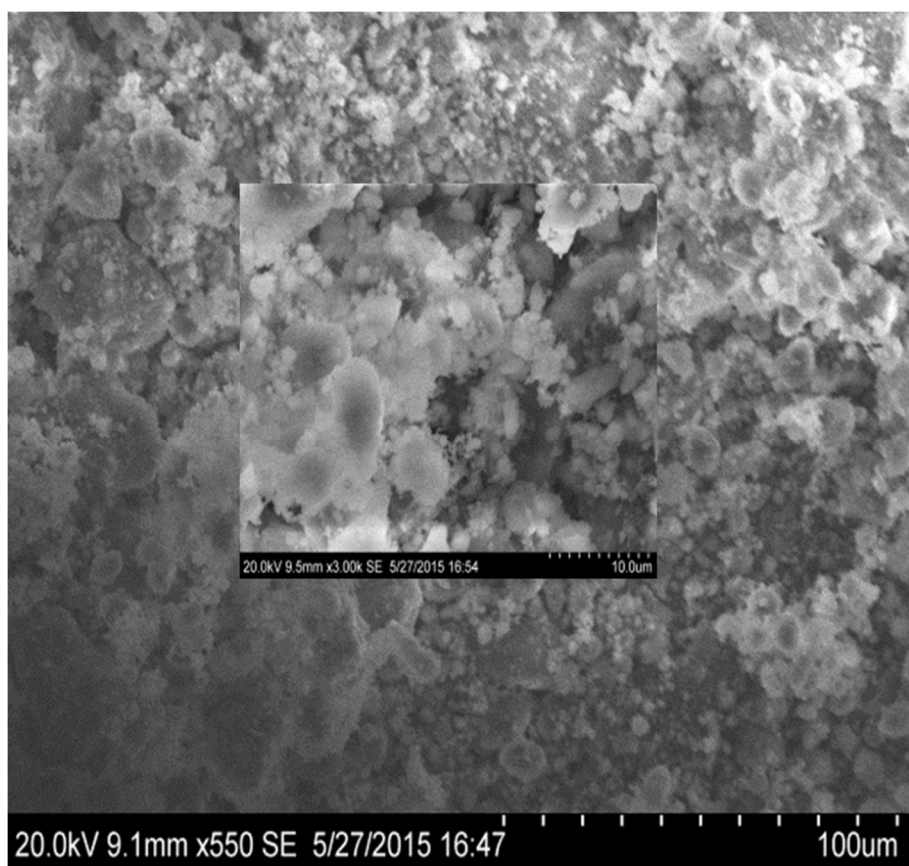


(b)

Fig.2. Particle size distribution analysis of kaolinite at different milling times (0h, 1h, 3h and 9h). (a) Size distribution, (b) Median particle size D50%.



(a)

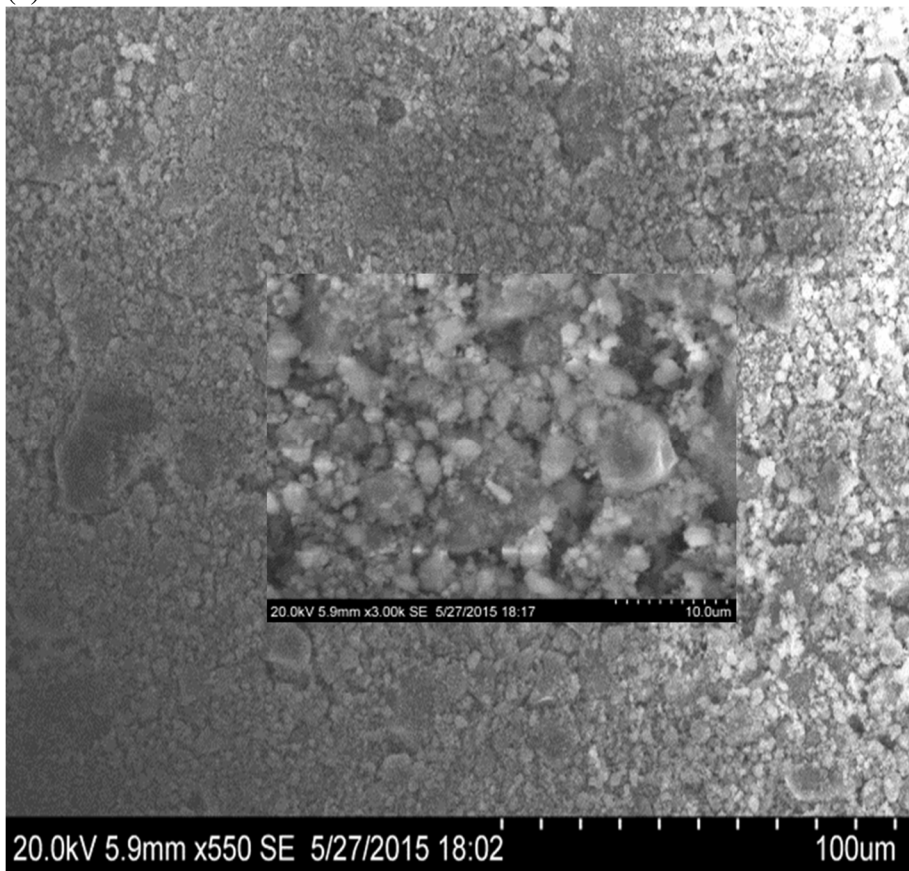


(b)

Fig. 3. SEM images of kaolinite at different milling stages: (a) Raw, (b) 1 h, (c) 3h, (d) 9 h.

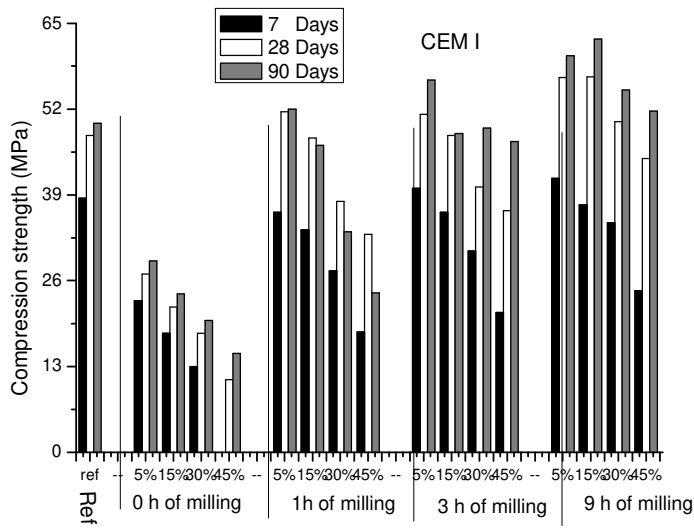


(c)

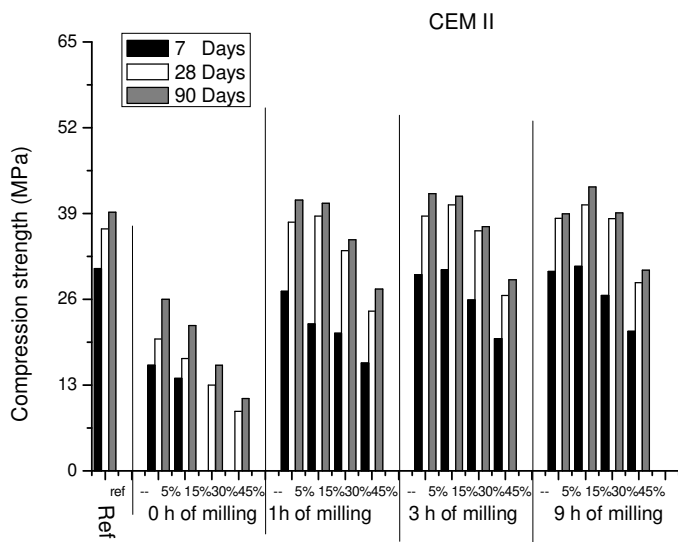


(d)

Figure 3. (Continued).

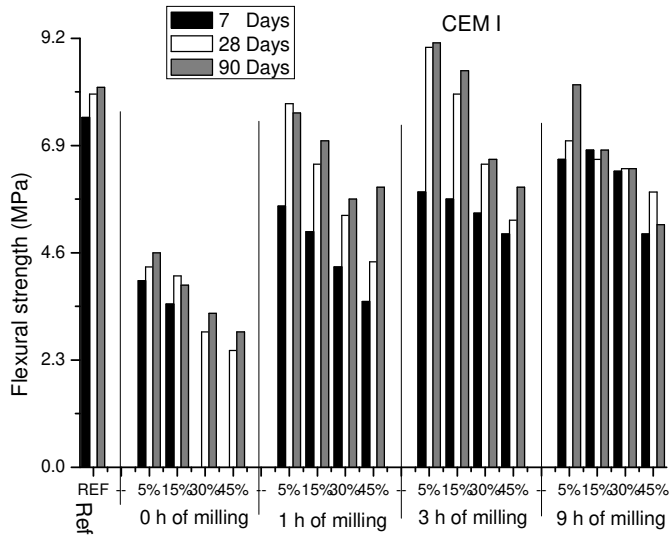


(a)

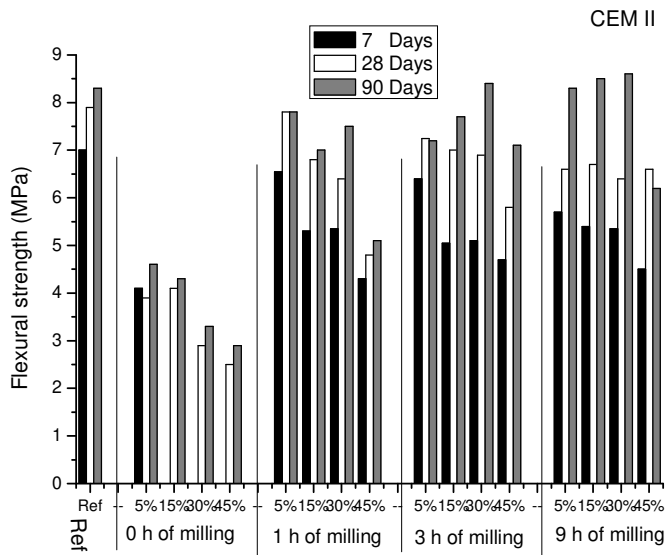


(b)

Fig. 4 The evolution of compressive strength (a) CEM I, (b) CEM II as function of substitution rate for mortars.

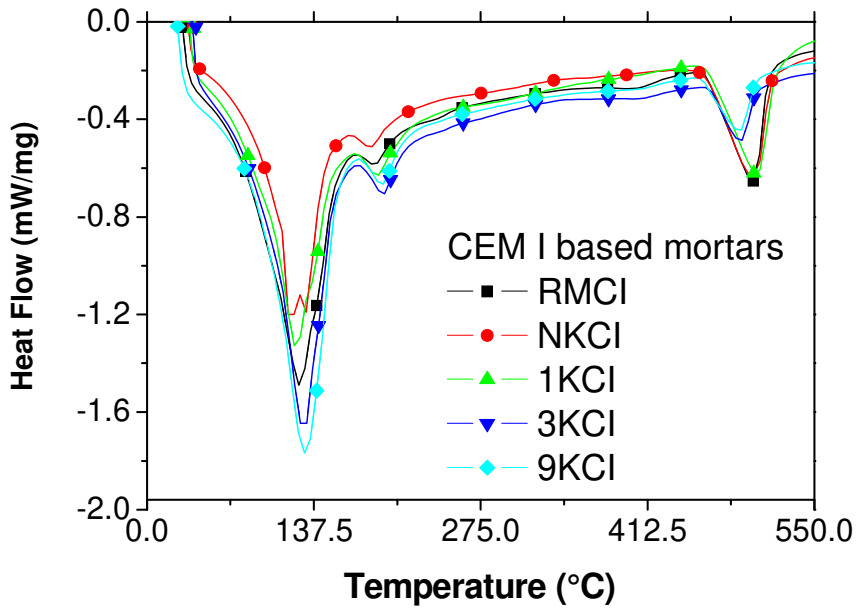


(a)

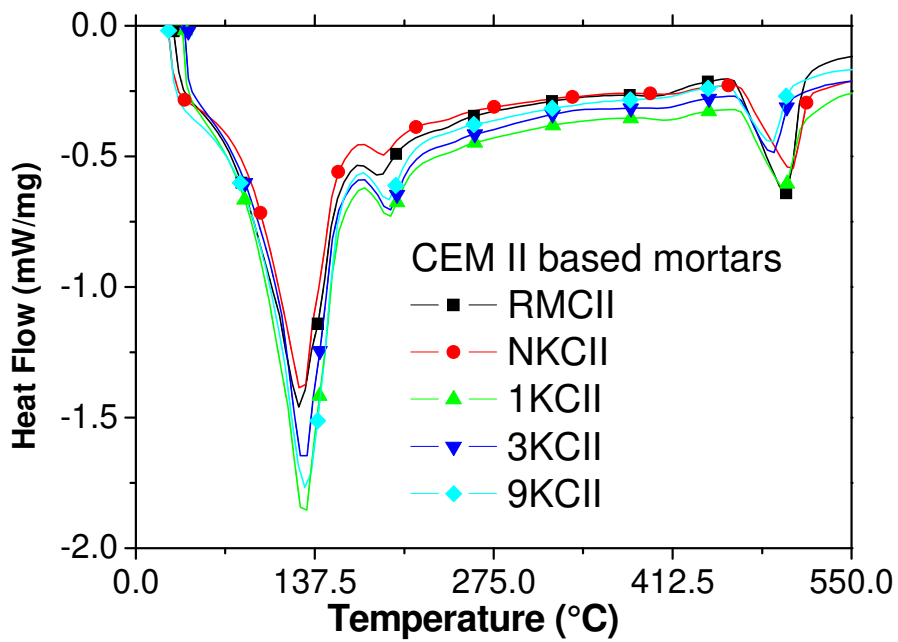


(b)

Fig. 5 The evolution of flexural strength (a) CEM I, (b) CEM II as function of substitution rate for mortars.



(a)



(b)

Fig. 6. DSC curves of hardened mortars at 90 days. (a) 15% kaolinite+ 85% CEM I, (b) 15% kaolinite+ 85% CEM II.

Table.1 Chemical composition of proclay kaolinite powder.

Species	Weight content (%)
SiO ₂	68.58
Al ₂ O ₃	27.23
TiO ₂	1.71
Fe ₂ O ₃	1.07
K ₂ O	0.55
CaO	0.38
MgO	0.12
Others	0.36

Table. 2 Decomposition enthalpy of C-A-H, C-S-H and Ca (OH)₂ of substituted (CEM I, CEM II) mortar at 15% of kaolinite at 90 curing days.

Formulation	CEM grade	Kaolinite	100°C-175°C	175°C-225°C	450°C – 525°C
			ΔH (J/g)	ΔH (J/g)	Ca(OH) ₂ ΔH (J/g)
RMCI	CEM I	None	-62.5	-11.3	-45.3
NKCI	CEM I	Natural	-56.3	-10.1	-46.1
1KCI	CEM I	Milled, 1h	-58.8	-12.5	-46.2
3KCI	CEM I	Milled, 3h	-86.3	-14.1	-15.5
9KCI	CEM I	Milled, 9h	-84.8	-13.6	-16.3
RMCI	CEM II	None	-56.1	-9.2	-40.1
NKCI	CEM II	Natural	-53.5	-7.8	-38.9
1KCI	CEM II	Milled, 1h	-81.2	-11.5	-25.2
3KCI	CEM II	Milled, 3h	-77.4	-13.2	-16.5
9KCI	CEM II	Milled, 9h	-79.3	-13.9	-15.3